Two-Stage pH Response of Poly(4-vinylpyridine) Grafted Gold Nanoparticles

Dongxiang Li,[†] Qiang He,[†,‡] Yang Yang,[‡] Helmuth Möhwald,[†] and Junbai Li*[,‡]

Max Planck Institute of Colloids and Interfaces, D-14476 Golm/Potsdam, Germany, and Beijing National Laboratory for Molecular Sciences (BNLMS), International Joint Laboratory, Institute of Chemistry, Chinese Academy of Sciences, Beijing 100080, P.R. China

Received April 22, 2008
Revised Manuscript Received July 24, 2008

Polymer brushes have attracted much attention because the polymer tailored surface has desirable energetic, mechanical, and electrical functionalities.[1] Many dense polymer brushes are covalently attached on various surfaces by the "grafting-from" strategy,[2] and recently the surface-initiated atom-transfer radical polymerization (ATRP) has become a popular method in the fabrication of various polymer brushes on planar and spherical surfaces.[3] In polymer physics, the responsive polymer chains will undergo a reversible conformational transition from a good solvent to a bad solvent at the "so-called" cloud point.[4] For example, water below 32 °C is a good solvent for the thermosensitive poly(*N*-isopropylacrylamide); the polymer chains under this condition are hydrated and adopt a random coiled conformation.[5] However, water becomes a poor solvent above 32 °C, where the polymer chains are dehydrated and turn into a globular conformation. Therefore, when the polymer chains are tethered on a solid surface as a polymer brush, the conformational transition will result in an adjustable property of the solid surface,[6] which can be used to construct intelligent micro- or nanodevices.[7]

For the pH-sensitive polymer poly(4-vinylpyridine) (PVP), the pH value may be considered as an effective parameter which influences the solvent quality. Previously, we reported the preparation and pH response of the gold/PVP nanocomposites.[8] The surface plasmon resonance (SPR) response showed a red shift of about 25 nm from low pH to neutral conditions. Basically, the agglomeration of gold nanoparticles shortens the distance between the gold cores, and this results in a red shift of SPR.[9] On the other hand, when the polymer layer collapses onto the gold cores, the increase of the refractive index around gold will also cause a red shift.[10] But how these two factors contribute to such a pH response is not clear because in the previous work the nanocomposite samples were prepared by incubating the nanocomposite sediments with dilute HCl solution of different pH, and hence the contribution from the polymer collapse could not be observed. Herein, in order to differentiate these two factors, the separated gold/PVP nanocomposites after ATRP were redispersed in dilute hydrochloric acid solution of pH 3.1 and purified to remove the residual DMF. Then, the concentrated nanocomposite suspension at pH 3.1 was quantitatively diluted by hydrochloric acid solutions at low pH values and neutral water or/and dilute basic solution to obtain the nanocomposite suspensions at different pH (Supporting Information). The detailed investigation shows that the gold/PVP nanocomposites have a two-stage response to the pH change; the polymer's stimuli-responsive collapse and the nanocomposite agglomeration give a contribution to the SPR shift in each stage.

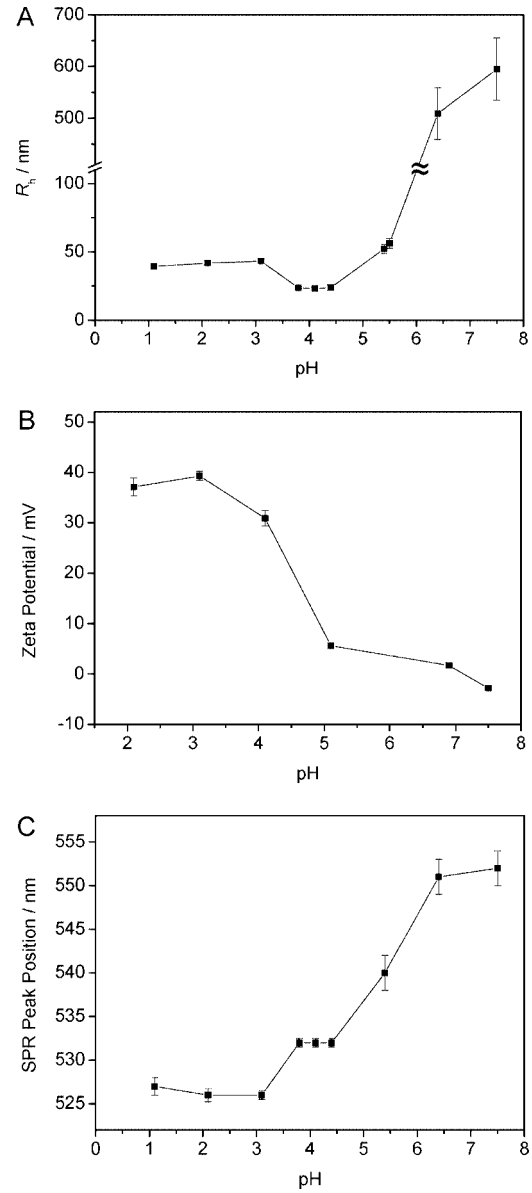

Figure 1. Hydrodynamic radius R_h (A), zeta potential (B), and surface plasmon resonance (SPR) (C) changes of the gold/PVP nanocomposites at different pH. The error bars indicate a deviation above and below the average of more than three separate measurements, and a scale break is included in the vertical axis in (A).

Figure 1A shows the change of the composite nanoparticle size at different pH by the dynamic light scattering (DLS) measurements. The apparent equivalent hydrodynamic radius (R_h) below pH 3.1 is about 42 nm, while at pH 3.8−4.4 it decreases by about 50% to 22 nm. Moreover, the particle zeta potential shown in Figure 1B maintains a high value from pH 2.1 to pH 3.1 (>35 mV), and such a high zeta potential can be ascribed to the formation of pyridinium ions according to the analysis of nitrogen valency.[8] On the other hand, at pH 4.1 the high zeta potential value (about 30 mV) may only be attributed to the physical adsorption of H^+ ions by the pyridinyl nitrogen

* Corresponding author: Tel +86 10 82614087; Fax +86 10 82612629; e-mail: jbli@iccas.ac.cn.
[†] Max Planck Institute of Colloids and Interfaces.
[‡] Chinese Academy of Sciences.

10.1021/ma800894c CCC: $40.75
Published on Web 09/10/2008

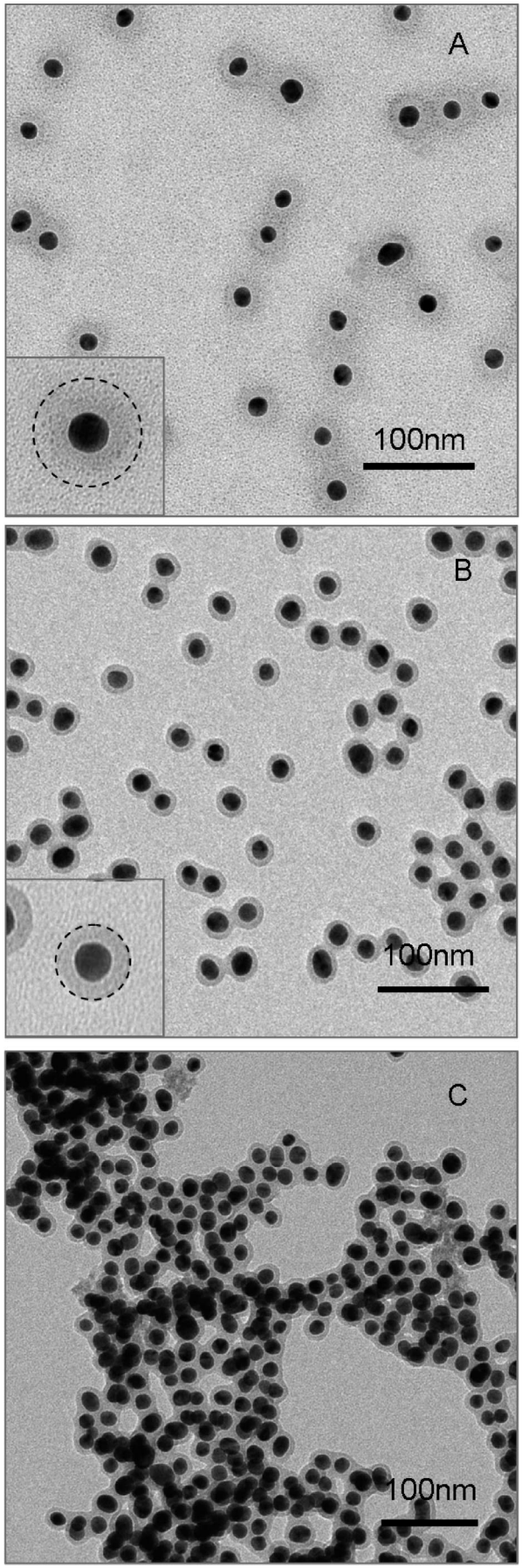

Figure 2. TEM images of the gold/PVP nanocomposites at pH 3.1 (A), pH 4.4 (B), and pH 7.5 (C). The inset in (A) or (B) shows one selected particle with larger magnification, and the dotted circle indicates a boundary of the polymer shell.

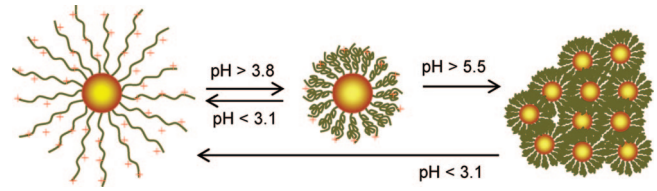

Figure 3. Scheme of the pH-responsive morphology change of the gold/PVP nanocomposites. The polymer chains are branched, and the whole particles are monodisperse and nonaggregated at low pH (<3.1); the polymer chains collapses onto the gold cores, but the whole particles are also monodisperse at a middle pH range (3.8−4.4); the whole particles agglomerate at higher pH (>5.5).

on the nanocomposite surface. Since the high zeta potential prevents the aggregation and thus lends monodispersity to the nanocomposites, so the R_h decrease from pH 3.1 to pH 3.8−4.4 can be ascribed to the collapse of polymer chains. However, at a higher pH (>5.1), the zeta potential drastically decreases and nearly turns into zero at neutral conditions. In this case, the colloidal particles may aggregate to large agglomerates, which is the reason for the particle size increase at high pH. In addition, it is found that the aggregate size at neutral conditions is not stable, and relatively stable data of R_h only can be obtained after 2 h. The agglomerates finally flocculate onto the tube wall after 2 days, whereas the flocculates can be easily redispersed in HCl solution at pH 3.1 because the pyridine groups are protonated again.

In the present work, because the suspension's pH is adjusted by a small step from a whole monodispersity, one can observe a red shift of the SPR in two stages, as shown in Figure 1C. At low pH (<3.1), the SPR peak is constant at about 527 nm, which implies monodisperse nanoparticles with extended polymer chains. From pH 3.1 to 3.8, a SPR red shift of about 5 nm occurs. It is reported that the polymer collapse around gold will change the refractive index of the gold surrounding and hence result in a red shift of gold SPR,[10] so this 5 nm red shift coincides with the polymer collapse as implied by DLS measurements. Subsequently, a plateau from pH 3.8 to 4.4 indicates that a stable monodisperse state can persist in a medium pH range although the PVP chains have collapsed. Upon further increasing the pH, another red shift of about 20 nm can be found with a broad SPR absorbance in the UV−vis spectra, and the SPR position is relatively stable around neutral conditions. It is known that the shortened distance of gold cores can result in a red shift of the gold SPR; hence, the later red shift can be ascribed to the nanocomposite agglomeration.[9] Additionally, the SPR red shift from the particle agglomeration is no larger than 20 nm, so the gold nanoparticles in the agglomerates are not closely aggregated due to the polymer's protection.

Figure 2A shows a typical TEM image at pH 3.1. It denotes that the gold/PVP nanoparticles are monodisperse, and a gold core is surrounded by a soft polymer layer with an average thickness of about 13.4 nm. However, as shown in Figure 2B, the polymer layer at pH 4.4 has a distinct boundary with a thickness of about 5.7 nm like a thin hard shell, while the nanocomposites remain monodisperse. Subsequently, at pH 7.5 large agglomerates are found as shown in Figure 2C, and it also denotes that the thickness of the polymer layer is similar to that at pH 4.4. Obviously, the TEM images directly display the pH response of the nanocomposites in accordance with the DLS and SPR results. Moreover, the polymer layer in Figure 2B can be considered as a bulk PVP shell because it collapses and is dried under vacuum. From the polymer thickness, the

graft density of the polymer brush can be estimated to be 0.19 chains/nm^2 (Supporting Information), which is a value common for polymer brushes obtained by surface-initiated ATRP.[11]

Schematically, the pH-responsive morphology of the gold/PVP nanocomposites is illustrated in Figure 3. At pH < 3.1, PVP brush chains are positively charged due to the formation of pyridinium ions;[8] hence, water is a good solvent, the polymer chains extend maximally under the electrostatic repulsion, and these highly charged particles are monodisperse in the suspension. For pH 3.8−4.4, the pyridinium groups are readily deprotonized, water becomes a poor solvent, and the polymer chains are collapsed onto the gold cores, so the particle size decreases by about 50%. Nevertheless, the physical adsorption of H^+ ions by the pyridinyl nitrogens on the nanocomposite surface maintains a high zeta potential; thus, the Coulomb repulsion makes the particles monodisperse. This response is reversible due to the protonation/deprotonation process of pyridine groups. For pH above 5.5, the very low concentration of H^+ ions results in a drastic decrease of the zeta potential and hence the nanocomposites aggregate. Thus, the large agglomerates are found by TEM, accompanied by the R_h increase in the DLS measurement. When the pH is adjusted from neutral to weakly acidic condition (pH 4−5), the H^+ adsorption on the surface of a whole large agglomerate apparently can not make itself into smaller ones and also cannot separate an aggregate into monodisperse particles with collapsed polymers. Therefore, the pH response from medium pH to neutral condition is not reversible. However, at pH 3.1 the reprotonation of pyridine groups on the polymer chains will transform the agglomerates into monodisperse particles. The pH response of the PVP brush also indicates that an intelligent polymer brush on gold nanoparticles obtained by ATRP should be able to induce a stimuli-responsive phase transition according to the solvent quality, which may be helpful to understand polymer brushes in more detail.

In this Note, summarily, the pH response of the PVP brush grafted gold nanoparticles is demonstrated to be a two-stage change in the hydrodynamic size, surface plasmon resonance, and TEM morphology. The two-stage red shift of the gold SPR response is ascribed to the polymer collapse and to the particle agglomeration. As to the potential uses, such intelligent polymer shell/inorganic core nanocomposites can be considered as building blocks to fabricate 2-D/3-D smart nanomaterials, which have potential for novel technological applications in biosensors and biotechnology.[12]

Acknowledgment. We acknowledge the financial support by the German Max-Planck Society and the Chinese Academy of Sciences. Q. He is grateful to the Alexander von Humboldt foundation for a research fellowship.

Supporting Information Available: Experimental details and calculation of the polymer graft density. This material is available free of charge via the Internet at http://pubs.acs.org.

References and Notes

(1) (a) Zhao, B.; Brittain, W. J. *Prog. Polym. Sci.* **2000**, *25*, 677. (b) Becer, C. R.; Haensch, C.; Hoeppener, S.; Schubert, U. S. *Small* **2007**, *3*, 220.
(2) (a) Weck, M.; Jackiw, J. J.; Rossi, R. R.; Weiss, P. S.; Grubbs, R. H. *J. Am. Chem. Soc.* **1999**, *121*, 4088. (b) Raula, J.; Shan, J.; Nuopponen, M.; Niskanen, A.; Jiang, H.; Kauppinen, E. I.; Tenhu, H. *Langmuir* **2003**, *19*, 3499. (c) Jordan, R.; West, N.; Chou, Y.-M.; Nuyken, O. *Macromolecules* **2001**, *34*, 1606.
(3) (a) Jones, D. M.; Smith, J. R.; Huck, W. T. S.; Alexander, C. *Adv. Mater.* **2002**, *14*, 1130. (b) Sanjuan, S.; Perrin, P.; Pantoustier, N.; Tran, Y. *Langmuir* **2007**, *23*, 5769. (c) Li, D. X.; He, Q.; Cui, Y.; Wang, K. W.; Zhang, X. M.; Li, J. B. *Chem.—Eur. J.* **2007**, *13*, 2224. (d) Ma, H. W.; Wells, M.; Beebe, T. P.; Chilkoti, A. *Adv. Funct. Mater.* **2006**, *16*, 640. (e) Li, D. X.; Cui, Y.; He, Q.; Wang, K. W.; Yan, X. H.; Li, J. B. *Adv. Funct. Mater.* **2007**, *17*, 3134. (f) Duan, H.; Kuang, M.; Wang, D.; Kurth, D. G.; Möhwald, H. *Angew. Chem., Int. Ed.* **2005**, *44*, 1717.
(4) (a) Baulin, V. A.; Halperin, A. *Macromol. Theory Simul.* **2003**, *12*, 549. (b) Baulin, V. A.; Zhulina, E. B.; Halperin, A. *J. Chem. Phys.* **2003**, *119*, 10977. (c) Afroze, F.; Nies, E.; Berghmans, H. *J. Mol. Struct.* **2000**, *554*, 55.
(5) (a) Wu, C.; Zhou, S. *Macromolecules* **1995**, *28*, 5388. (b) Schild, H. G. *Prog. Polym. Sci.* **1992**, *17*, 163.
(6) Kaholek, M.; Lee, W.-K.; Ahn, S.-J.; Ma, H. W.; Caster, K. C.; LaMattina, B.; Zauscher, S. *Chem. Mater.* **2004**, *16*, 3688.
(7) (a) Nath, N.; Chilkoti, A. *Adv. Mater.* **2002**, *14*, 1243. (b) Beebe, D. J.; Moore, J. S.; Yu, Q.; Liu, R. H.; Kraft, M. L.; Jo, B. H.; Devadoss, C. *Proc. Natl. Acad. Sci. U.S.A.* **2000**, *97*, 13488.
(8) Li, D. X.; He, Q.; Cui, Y.; Li, J. B. *Chem. Mater.* **2007**, *19*, 412.
(9) Weisbecker, C. S.; Merritt, M. V.; Whitesides, G. M. *Langmuir* **1996**, *12*, 3763.
(10) (a) Underwood, S.; Mulvaney, P. *Langmuir* **1994**, *10*, 3427. (b) Schmitt, J.; Machtle, P.; Eck, D.; Möhwald, H.; Helm, C. A. *Langmuir* **1999**, *15*, 3256.
(11) Plunkett, K. N.; Zhu, X.; Moore, J. S.; Leckband, D. E. *Langmuir* **2006**, *22*, 4259.
(12) (a) Binder, W. H. *Angew. Chem., Int. Ed.* **2005**, *44*, 5172. (b) Owens, D. E., III; Eby, J. K.; Jian, Y. C.; Peppas, N. A. *J. Biomed. Mater. Res. A* **2007**, *83A*, 692.

MA800894C